

Stabilization and Destabilization of the Ru–CO Bond During the 2,2'-Bipyridin-6-onato (bpyO)-Localized Redox Reaction of [Ru(terpy)(bpyO)(CO)](PF₆)

Takashi Tomon,^[a] Take-aki Koizumi,^[a] and Koji Tanaka*^[a]

Keywords: Carbonyl complex / Electrochemistry / IR spectroscopy / Ruthenium

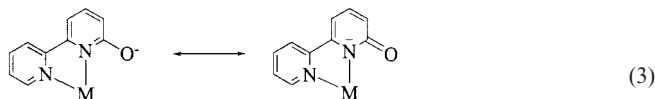
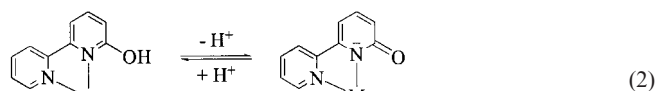
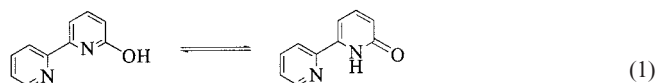
Two stereoisomers of [Ru(terpy)(bpyO)(CO)](PF₆) ([1]⁺ and [2]⁺; terpy = 2,2':6',2''-terpyridine, bpyO = 2,2'-bipyridin-6-onato) were prepared. The pyridonato moiety in the bpyO ligand of [1]⁺ and [2]⁺ is located *trans* and *cis*, respectively, to CO. Treatment of [1]⁺ and [2]⁺ with HPF₆ produced [1H]²⁺ and [2H]²⁺, both of which contain bpyOH (bpyOH = 6-hydroxy-2,2'-bipyridine). The difference in the pK_a values of [1H]²⁺ (3.5) and [2H]²⁺ (3.9) reflects the stronger electronic interaction between CO and the pyridonato moiety in the bpyO ligand in the *trans* position compared with that in the *cis* position. The molecular structures of [1](PF₆), [2](PF₆)·H₂O and [2H](PF₆)₂·2H₂O were determined by X-ray structure analyses. [1]⁺ and [2]⁺ undergo one, reversible reduction at E_{1/2} = −1.65 V and −1.51 V, respectively, and one

irreversible reduction at E_{p,c} = −2.07 and E_{p,c} = −2.13 V, respectively. Both reductions are assigned to redox reactions localized at the terpy and bpyO ligands. Irreversible reduction of [1]⁰ results from reductive cleavage of the Ru–CO bond of [1][−]. On the other hand, a two-electron oxidation of [2][−] almost regenerates [2]⁺ because of the depression of the reductive Ru–CO bond cleavage of [2][−] due to cyclometalation formed by an attack of oxygen of bpyO to the carbon of the Ru–CO bond. An unusually large shift of the ν(C≡O) band on going from [2]⁰ (1950 cm^{−1}) to [2][−] (1587 cm^{−1}) also supports a reversible cyclometalation driven by the bpyO-localized redox reaction.

© Wiley-VCH Verlag GmbH & Co. KGaA, 69451 Weinheim, Germany, 2005

Introduction

Polypyridylruthenium complexes exhibit a unique electrochemical behavior^[1] because of the low energy level of the π*-orbitals of the ligands. For example, redox reactions of polypyridyl ligands can be utilized as electron pools in photo-^[2] and electrochemical^[3] reduction of CO₂ catalyzed by polypyridylruthenium complexes. Modification of polypyridyl ligands may create new functionalities in addition to the role of the redox centers of ruthenium complexes. For example, a keto-enol tautomerism between 6-hydroxy-2,2'-bipyridine (bpyOH) and 2,2'-bipyridin-6(1H)-one (bpyO) [Equation (1)] would induce the acid-base equilibrium of bpyOH ligated to Ru [Equation (2)], followed by resonance between (2,2'-bipyridin-6-onato)- and (2,2'-bipyridin-6-olato)ruthenium complexes [Equation (3)].



A few metal complexes with bpyO have been reported to date,^[4] but neither the equilibrium of Equation (2) nor the resonance of Equation (3) has been discussed. The acid-base equilibrium of Ru(bpyOH) complexes [Equation (2)] and the subsequent resonance of Ru(bpyO) ones [Equation (3)] may allow these complexes to undergo proton-coupled electron transfer. The ligand-localized redox reaction of metal–bpyO(H) complexes would influence the equilibrium of Equation (2) and the resonance of Equation (3). In connection with this, a drastic change of basicity of the free nitrogen of the 1,8-naphthyridine ligand of [Ru(bpy)₂-(napy-κN)(CO)]²⁺ (napy = 1,8-naphthyridine) has been reported. One-electron reduction of napy resulted in an attack of the free nitrogen at the carbon atom of the Ru–CO bond to form a metallacyclic ring, which smoothly opened upon oxidation of the napy ligand.^[5] Such reversible cyclometalation driven by ligand-localized redox reactions falls

^[a] Institute for Molecular Science and CREST, Japan Science and Technology Agency (JST), 5-1 Higashi-yama, Myodai-ji, Okazaki, Aichi 444-8787, Japan
Fax: + 81-564-59-5582

E-mail: ktanaka@ims.ac.jp

Supporting information for this article is available on the WWW under <http://www.eurjic.org> or from the author.

into a new category in a number of metallacyclic complexes bearing five-^[6] and six- membered^[7] rings and containing CO as a cycle component.

In this work, we have prepared two geometrical isomers of $[\text{Ru}(\text{terpy})(\text{bpyO})(\text{CO})]^+$ with regard to the orientation of bpyO ($[\mathbf{1}]^+$ and $[\mathbf{2}]^+$) and determined the $\text{p}K_{\text{a}}$ values of their protonated complexes ($[\mathbf{1H}]^{2+}$ and $[\mathbf{2H}]^{2+}$). Two-electron reduction of $[\mathbf{1}]^+$, which has the pyridonato moiety of the bpyO ligand *trans* to CO, caused reductive cleavage of the Ru–CO bond, while two-electron reduction of $[\mathbf{2}]^+$, which has the pyridonato moiety of the bpyO ligand *cis* to CO, formed a metallacyclic ring due to an attack of the oxygen of bpyO at the carbon of the Ru–CO bond.

Results and Discussion

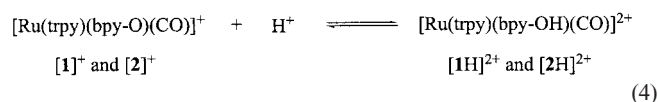
Syntheses and Structures of $[\mathbf{1}]^+$, $[\mathbf{1H}]^{2+}$, $[\mathbf{2}]^+$, and $[\mathbf{2H}]^{2+}$

There are two possible orientations of the pyridonato ring of bpyO in $[\text{Ru}(\text{terpy})(\text{bpyO})(\text{CO})]^+$ (vide infra): one is in a position *trans* to CO ($[\mathbf{1}]^+$) and the other is in a position *cis* to CO ($[\mathbf{2}]^+$). The preparative pathways of $[\mathbf{1}]^+$ and $[\mathbf{2}]^+$ are depicted in Scheme 1. Treatment of $[\text{RuCl}(\text{terpy})(\text{bpyOH})]^+$ with AgPF_6 under CO (15 atm) in 2-methoxyethanol produced $[\text{Ru}(\text{terpy})(\text{bpyO})(\text{CO})]^+$ ($[\mathbf{1}]^+$).

The ^1H NMR spectra of the PF_6 salt of $[\mathbf{1}]^+$ clearly show the selective formation of one of the two isomers under these reaction conditions. X-ray analysis of $[\mathbf{1}](\text{PF}_6)$ demonstrated coordination of CO to Ru in the position *trans* to the pyridonato ring of bpyO (vide infra). On the other hand, the substitution reaction of an aqua ligand of $[\text{Ru}(\text{terpy})(\text{bpyO})(\text{OH}_2)]^+$ by CO (20 atm) in 2-methoxyethanol selectively produced the other isomer of $[\text{Ru}(\text{terpy})(\text{bpyO})(\text{CO})]^+$ with CO in the position *cis* to the pyridonato ring of bpyO ($[\mathbf{2}]^+$). The ^1H NMR spectra of the crude product of $[\mathbf{2}](\text{PF}_6)$ did not show any contamination by $[\mathbf{1}](\text{PF}_6)$. It is worthwhile to note that the orientation of bpyOH in $[\text{Ru}(\text{terpy})(\text{bpyOH})\text{Cl}]^+$ is inverted in $[\mathbf{1}]^+$, whereas that in $[\text{Ru}(\text{terpy})(\text{bpyO})(\text{OH}_2)]$ is maintained in $[\mathbf{2}]^+$. Such a difference may result from an involvement of an attack of CO to pentacoordinate

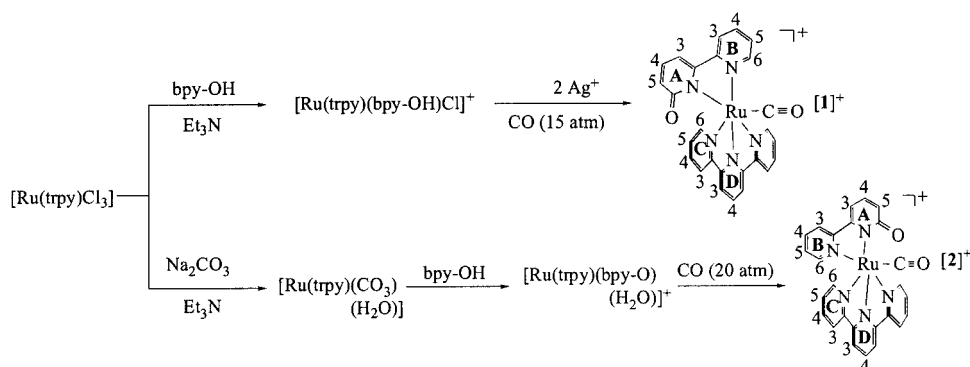
$[\text{Ru}(\text{terpy})(\text{bpyOH})]^+$ that would be produced in the reaction of $[\text{Ru}(\text{terpy})(\text{bpyOH})\text{Cl}]^+$ with Ag^+ .

Treatment of $[\mathbf{1}]^+$ and $[\mathbf{2}]^+$ with one equivalent of HPF_6 produced $[\mathbf{1H}]^{2+}$ and $[\mathbf{2H}]^{2+}$, respectively, in CH_3CN . The addition of one equivalent of Et_3N to $[\mathbf{1H}]^{2+}$ and $[\mathbf{2H}]^{2+}$ completely regenerated $[\mathbf{1}]^+$ and $[\mathbf{2}]^+$, respectively, in CH_3CN [Equation (4)].



The ^1H NMR spectra of $[\mathbf{1}]^+$ and $[\mathbf{2}]^+$ clearly confirm the protonation of the oxygen atom of the bpyO ligand, since treatment of $[\mathbf{1}]^+$ and $[\mathbf{2}]^+$ with HPF_6 in CD_3CN shifts the pyridonate ring protons to lower magnetic field by 0.65–1.3 ppm, while the terpy and pyridine protons of bpyO shift by only 0.1–0.25 ppm upon protonation of $[\mathbf{1}]^+$ and $[\mathbf{2}]^+$. The $\text{p}K_{\text{a}}$ values of hydroxypyridine in $[\mathbf{1H}](\text{PF}_6)_2$ and $[\mathbf{2H}](\text{PF}_6)_2$ were determined to be 3.5 and 3.9, respectively, by pH titrations in H_2O at 25 °C. The difference in the $\text{p}K_{\text{a}}$ values of $[\mathbf{1H}]^{2+}$ and $[\mathbf{2H}]^{2+}$ can reasonably be ascribed to the stronger electronic interaction between CO and the pyridonato moiety in the bpyO ligand in the *trans* position compared with that in the *cis* position.

The crystal structures of the cations of complexes $[\text{Ru}(\text{terpy})(\text{bpyO})(\text{OH}_2)](\text{PF}_6)$ and $[\text{Ru}(\text{terpy})(\text{bpyOH})\text{Cl}](\text{PF}_6)$ ^[8] are depicted in Figure 1 and the Supporting Information, respectively. The bond lengths and angles of $[\text{Ru}(\text{terpy})(\text{bpyO})(\text{OH}_2)]^+$ are listed in Table 1. The pyridonato ring of $[\text{Ru}(\text{terpy})(\text{bpyO})(\text{OH}_2)]^+$ and the hydroxypyridine ring of $[\text{Ru}(\text{terpy})(\text{bpyOH})\text{Cl}]^+$ are situated *cis* to the H_2O and Cl ligands, respectively. The C1–O1 and C–C bonds lengths of the pyridonato ring of bpyO in $[\text{Ru}(\text{terpy})(\text{bpyO})(\text{OH}_2)]^+$ are 1.288(5) Å and 1.368(7)–1.417(7) Å, and are similar to those in the 2-pyridonato ligands of $[\text{Ru}(\text{terpy})(\text{NC}_5\text{H}_4\text{O}-\kappa\text{N})_2(\text{OH}_2)]$ ^[9] and *mer*- $[\text{Pt}(\text{NH}_3)_2(\text{NC}_5\text{H}_4\text{O}-\kappa\text{N})\text{Cl}_3]$ ^[10] ($\text{NC}_5\text{H}_4\text{O}-\kappa\text{N}$ = 2-pyridonato). The Ru1–O2 bond length is 2.152(3) Å, which is quite close to that in $[\text{Ru}(\text{terpy})(\text{NC}_5\text{H}_4\text{O}-\kappa\text{N})_2(\text{OH}_2)]$ (2.160 Å).^[9] The interatomic O1...O2 distance [2.533(5) Å] be-



Scheme 1. Synthetic routes to the carbonyl complexes $[\mathbf{1}]^+$ and $[\mathbf{2}]^+$

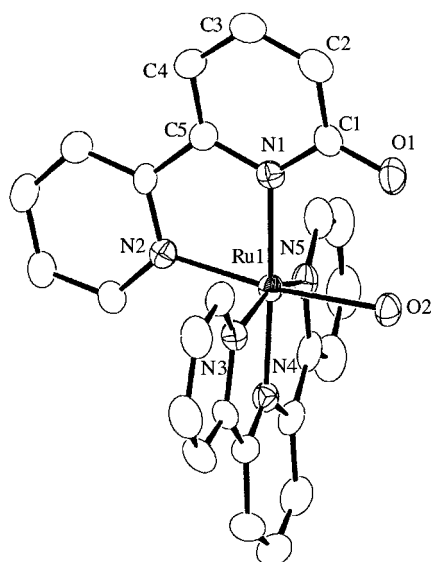


Figure 1. Molecular structure of $[\text{Ru}(\text{terpy})(\text{bpyO})(\text{OH}_2)]^+$ with atom labeling; hydrogen atoms are omitted for simplicity

Table 1. Selected bond lengths [\AA] and angles [$^\circ$] for $[\text{Ru}(\text{terpy})-(\text{bpyO})(\text{OH}_2)](\text{PF}_6)$

| | | | |
|-----------|----------|-----------|----------|
| Ru1–N1 | 2.089(4) | Ru1–N2 | 2.036(4) |
| Ru1–N3 | 2.062(4) | Ru1–N4 | 1.957(4) |
| Ru1–N5 | 2.081(4) | Ru1–O2 | 2.152(3) |
| N1–C1 | 1.370(6) | N1–C5 | 1.358(6) |
| C1–O1 | 1.288(5) | C1–C2 | 1.417(7) |
| C2–C3 | 1.368(7) | C3–C4 | 1.399(7) |
| C4–C5 | 1.375(6) | | |
| N1–Ru1–N2 | 78.7(1) | N1–Ru1–N4 | 175.8(1) |
| N1–Ru1–O2 | 94.5(1) | N3–Ru1–N4 | 80.0(2) |
| N4–Ru1–N5 | 79.6(2) | | |
| O1–C1–N1 | 120.1(4) | O1–C1–C2 | 120.8(4) |
| N1–C1–C2 | 119.1(4) | | |

tween the pyridonato and the aqua ligands suggests hydrogen-bond formation between them.

The molecular structures of the ruthenium carbonyl complexes bearing bpyO ($[1]^+$ and $[2]^+$) and bpyOH ($[2\text{H}]^{2+}$) were determined by X-ray crystal structure analysis. The crystal structures of the cations of these complexes are shown in Figure 2; selected bond lengths and angles are listed in Table 2. The pyridonato group of the bpyO ligand in $[1]^+$ and $[2]^+$ is situated *trans* and *cis*, respectively, to the CO ligand (Figure 2a and 2b). The orientation of bpyOH in $[2\text{H}]^{2+}$ is the same as that in $[2]^+$ (Figure 2c). The Ru1–N bond lengths of terpy in the carbonyl complexes are 1.989(3)–2.100(3) for $[1]^+$, 2.006(9)–2.09(1) for $[2]^+$, and 1.983(4)–2.098(4) for $[2\text{H}]^{2+}$. These bond lengths are close to those of similar ruthenium carbonyl complexes such as $[\text{Ru}(\text{terpy})(\text{bpy})(\text{CO})]^{2+}$ (1.989–2.086 \AA)^[3c] and $[\text{Ru}(\text{terpy})(\text{bpy})(\text{py})]^{2+}$ (1.963–2.078 \AA ; py = pyridine).^[11] The C1–O1 bond lengths of bpyO in $[1]^+$ [1.250(4) \AA] and $[2]^+$ [1.26(1) \AA] are in the range of a normal C=O double bond. It is worthwhile to note that the C1–O1 bond length in $[2\text{H}]^{2+}$ [1.326(7) \AA] is much longer than those in $[1]^+$ and $[2]^+$, and is close to that of a C–O single bond. Further-

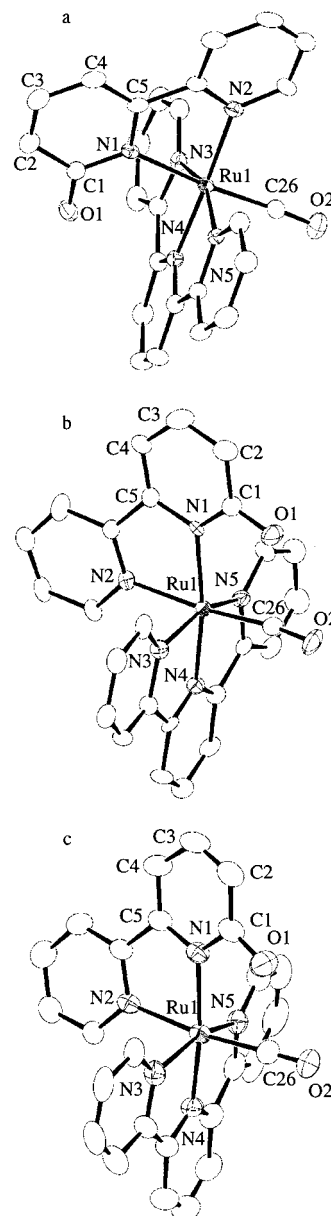


Figure 2. Molecular structures of $[1]^+$ (a), $[2]^+$ (b) and $[2\text{H}]^{2+}$ (c) with atom labeling; hydrogen atoms are omitted for simplicity

more, elongation of the Ru1–N1 bond length [2.112(4) \AA], as well as the C1–O1 bond length of $[2\text{H}]^{2+}$, compared with that of $[2]^+$ [2.087(9) \AA] demonstrates the decrease of the covalency of the Ru–N1 bond due to the protonation of the oxygen atom of bpyO in $[2]^+$ [Equation (2)]. There seems to be a substantial strain in the coordination of bpyO to Ru in $[1]^+$ because the C1–N1–Ru1–N4 dihedral angle [15.6(3) $^\circ$] in $[1]^+$ is much larger than the corresponding angle (C1–N1–Ru1–C26) in $[2]^+$ [7(1) $^\circ$]. This may be caused by repulsion between the lone-pair electrons of the bpyO oxygen atom and the π -electrons of the central pyridine ring of terpy. The shift of the oxygen atom of bpyO near the pyridyl ring of terpy in $[1]^+$ to the position *cis* to the CO ligand of $[2]^+$ will release the strain in the coordination of bpyO to Ru. A relatively short interatomic distance between

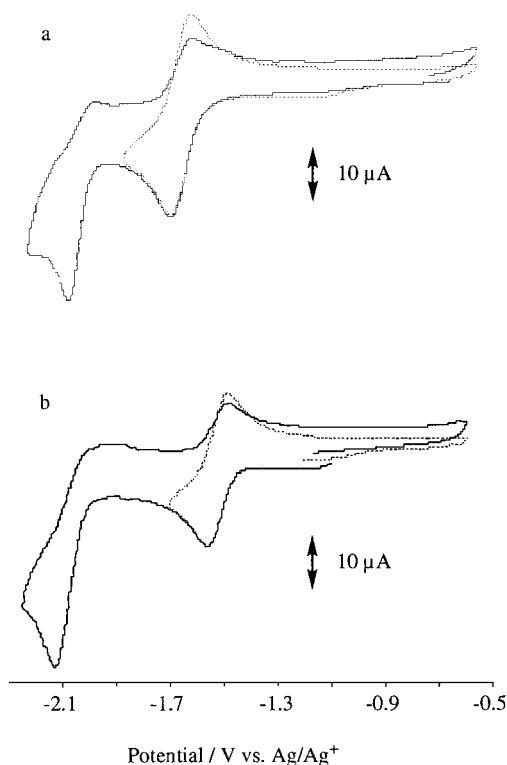
Table 2. Selected bond lengths [Å] and angles [°] for [1](PF₆), [2](PF₆)·H₂O, and [2H](PF₆)₂·2H₂O

| [1] ⁺ | | | |
|--------------------|----------|------------|----------|
| Ru1–N1 | 2.118(3) | R1–N2 | 2.086(3) |
| Ru1–N3 | 2.085(3) | Ru1–N4 | 1.989(3) |
| Ru1–N5 | 2.100(3) | Ru1–C26 | 1.868(3) |
| N1–C1 | 1.382(4) | N1–C5 | 1.373(4) |
| C1–O1 | 1.250(4) | C1–C2 | 1.441(5) |
| C2–C3 | 1.355(5) | C3–C4 | 1.404(5) |
| C4–C5 | 1.376(5) | C26–O2 | 1.137(4) |
| N1–Ru1–N2 | 77.6(1) | N1–Ru1–N4 | 98.6(1) |
| N2–Ru1–C26 | 97.2(1) | N3–Ru1–N4 | 79.7(1) |
| N4–Ru1–N5 | 79.3(1) | Ru1–C26–O2 | 176.0(3) |
| O1–C1–N1 | 120.4(3) | O1–C1–C2 | 122.3(3) |
| N1–C1–C2 | 117.2(3) | | |
| [2] ⁺ | | | |
| Ru1–N1 | 2.087(9) | R1–N2 | 2.13(1) |
| Ru1–N3 | 2.08(1) | Ru1–N4 | 2.006(9) |
| Ru1–N5 | 2.09(1) | Ru1–C26 | 1.90(1) |
| N1–C1 | 1.33(1) | N1–C5 | 1.40(1) |
| C1–O1 | 1.26(1) | C1–C2 | 1.40(2) |
| C2–C3 | 1.39(2) | C3–C4 | 1.40(2) |
| C4–C5 | 1.35(2) | C26–O2 | 1.12(1) |
| N1–Ru1–N2 | 78.3(4) | N1–Ru1–C26 | 96.2(4) |
| N2–Ru1–N4 | 93.6(4) | N3–Ru1–N4 | 79.1(4) |
| N4–Ru1–N5 | 78.4(4) | Ru1–C26–O2 | 173(1) |
| O1–C1–N1 | 120(1) | O1–C1–C2 | 120(1) |
| N1–C1–C2 | 120(1) | | |
| [2H] ²⁺ | | | |
| Ru1–N1 | 2.112(4) | R1–N2 | 2.117(5) |
| Ru1–N3 | 2.098(4) | Ru1–N4 | 1.983(4) |
| Ru1–N5 | 2.094(4) | Ru1–C26 | 1.909(6) |
| N1–C1 | 1.345(7) | N1–C5 | 1.366(7) |
| C1–O1 | 1.326(7) | C1–C2 | 1.410(8) |
| C2–C3 | 1.344(9) | C3–C4 | 1.399(9) |
| C4–C5 | 1.366(7) | C26–O2 | 1.115(7) |
| N1–Ru1–N2 | 77.3(2) | N1–Ru1–C26 | 96.6(2) |
| N2–Ru1–N4 | 93.8(2) | N3–Ru1–N4 | 79.2(2) |
| N4–Ru1–N5 | 79.1(2) | Ru1–C26–O2 | 177.5(5) |
| O1–C1–N1 | 116.5(5) | O1–C1–C2 | 122.0(5) |
| N1–C1–C2 | 121.4(5) | | |

the oxygen atom of bpyO and the carbon atom of CO in [2]⁺ of 2.55 Å implies a donor–acceptor interaction between them. An increase of the distance between the oxygen atom of bpyOH and the carbon atom of CO (O1...C26 = 2.62 Å) in [2H]²⁺ is therefore explained by the decrease in the basicity of the oxygen atom of bpyO upon protonation.

Cyclic Voltammetry of [1](PF₆), [2](PF₆), [1H](PF₆)₂ and [2H](PF₆)₂

The cyclic voltammograms (CVs) of [1](PF₆) and [2](PF₆) were measured in CH₃CN (Figure 3). The CV of [1]⁺ shows a nearly reversible redox couple at $E_{1/2} = -1.65$ V ($E_{p,c} = -1.70$, $E_{p,a} = -1.61$ V) and a subsequent irreversible cathodic wave at $E_{p,c} = -2.07$ V (Figure 3a), both of which are assigned to terpy- and bpyO-ligand-based redox reactions^[12] by analogy with the redox behavior of

Figure 3. Cyclic voltammograms of [1](PF₆) (a) and [2](PF₆) (b) in CH₃CN under N₂; dE/dt = 100 mV·s⁻¹

[Ru(terpy)₂]²⁺.^[13] The irreversible reduction of [1]⁰ probably results from a partial Ru–CO bond cleavage of [1][–] (vide infra), because two-electron reduction of [Ru(terpy)(bpy)(CO)]²⁺ leads to reductive Ru–CO bond cleavage (CO evolution), which is a key process in the electrochemical reduction of CO₂ catalyzed by this complex.^[3e] The CV of [2]⁺ also shows an almost reversible [2]⁺/[2]⁰ redox couple at $E_{1/2} = -1.51$ V ($E_{p,c} = -1.55$ and $E_{p,a} = -1.47$ V) and an irreversible cathodic wave at $E_{p,c} = -2.13$ V (Figure 3b). In contrast to the reductive cleavage of the Ru–CO bond of [1][–], the irreversible reduction of [2]⁰ is due to a cyclometalation caused by an intramolecular attack of the pyridonato oxygen at the carbonyl carbon atom (vide infra). The oxidation processes of [1]⁺ and [2]⁺ were also examined, but both complexes were not oxidized up to +1.0 V.

The CV of [1H]²⁺ in CH₃CN displays four cathodic waves at $E_{p,c} = -1.40$, -1.69 , -1.85 , and -2.05 V in the first potential sweep (Figure 4a).^[14] The cathodic wave at $E_{p,c} = -1.40$ V completely disappeared in the second potential sweep, while the other three cathodic waves at $E_{p,c} = -1.69$, -1.85 , and -2.05 V remained at almost the same potentials in multiscanning potential sweeps. The addition of one equivalent of Et₃N to the solution also caused the disappearance of the cathodic wave at $E_{p,c} = -1.40$ V in the first potential sweep. However, the second cathodic wave became broad. Based on the fact that Et₃NH⁺ undergoes an irreversible reduction at -1.75 V in CH₃CN on a glassy carbon electrode, the broad cathodic wave at $E_{p,c} = -1.69$ V apparently results from overlapping of the terpy-

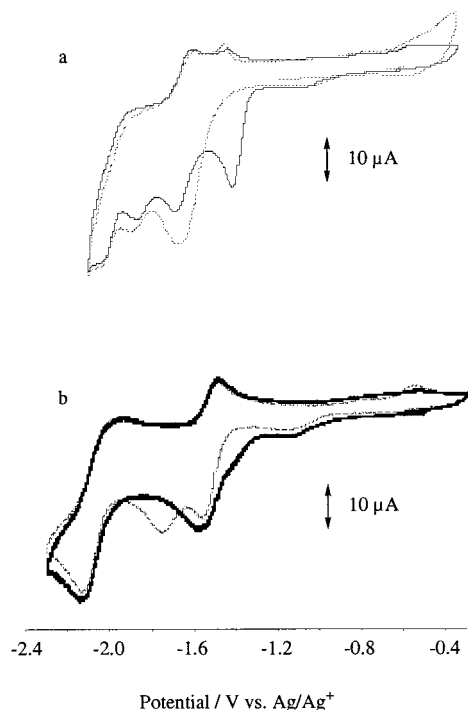
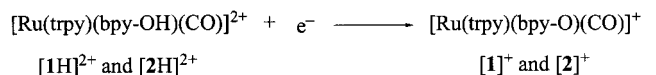


Figure 4. Cyclic voltammograms of [1H](PF₆)₂ (a) and [2H](PF₆)₂ (b) in the absence (—) and the presence (---) of 1.0 equiv. of Et₃N under N₂; dE/dt = 100 mV·s⁻¹

based reduction and an irreversible reduction of Et₃NH⁺ produced in the reaction of [1H]⁺ with Et₃N. The CV of [2H]²⁺ displays a broad cathodic wave at $E_{p,c} = -1.58$ V and a subsequent irreversible cathodic wave at $E_{p,c} = -2.14$ V (Figure 4b).^[15] Addition of one equivalent of Et₃N to the solution sharpened the cathodic wave at $E_{p,c} = -1.58$ V and resulted in an irreversible cathodic wave at -1.75 V due to the reduction of Et₃NH⁺. These results indicate that the proton of the bpyOH ligand of [1H]²⁺ and [2H]²⁺ undergoes irreversible reduction at $E_{p,c} = -1.40$ and -1.58 V, respectively, to form [1]⁺ and [2]⁺ [Equation (5)].

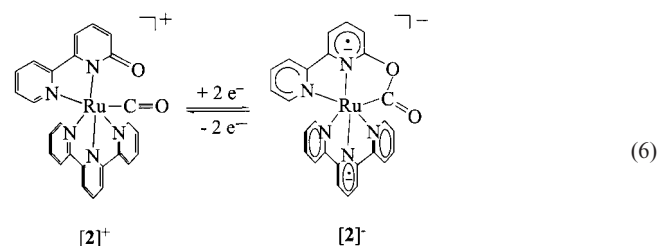


IR Spectroscopy of [1]⁺ and [2]⁺ under the Electrolysis Conditions

The IR spectra of [1](PF₆) show the $\nu(\text{C}\equiv\text{O})$ band and the $\nu(\text{C}=\text{O})$ band of bpyO at 1979 and 1620 cm⁻¹, respectively, in CD₃CN. The appearance of those bands at 1996 and 1612 cm⁻¹ in the IR spectrum of [2](PF₆) is ascribed to the stronger electron-donor ability of bpyO located *trans* to CO compared to when it is *cis* to CO (the redox potentials of the reversible [1]^{+/0} and [2]^{+/0} couples were observed at -1.65 and -1.51 V, respectively, in CH₃CN). In other words, the resonance between metal pyridinolates and pyridonate forms of [1]⁺ [Equation (3)] is shifted more towards the pyridonate than in [2]⁺. It is worthwhile to note that

the redox behaviors of [1]⁺ and [2]⁺ are similar (one reversible and one irreversible reduction). However, there is a distinct difference between the IR spectra during the reduction and oxidation cycles of the two complexes. The $\nu(\text{C}\equiv\text{O})$ band of [1]⁺ at 1979 cm⁻¹ disappears completely during the controlled potential electrolysis of the complex at -1.70 V in CH₃CN, and a new $\nu(\text{C}\equiv\text{O})$ band appears at 1932 cm⁻¹ (Figure 5a). The 1932 cm⁻¹ band is further shifted to 1853 cm⁻¹, with a lower peak intensity, when the electrolysis potential is changed from -1.70 V to -2.0 V (Figure 5b). The decrease of the peak intensity of the 1853 cm⁻¹ band compared with those of the 1979 and 1932 cm⁻¹ bands probably results from a gradual Ru–CO bond cleavage of [1]⁺; reoxidation of the solution at 0 V did not recover the peak intensity of the $\nu(\text{C}\equiv\text{O})$ band of [1]⁺ at 1979 cm⁻¹. Besides the change of the $\nu(\text{C}\equiv\text{O})$ band, two bands at 1605 and 1620 cm⁻¹, assigned to the stretching modes of the pyridine rings and the C=O group of the bpyO ligand of [1]⁺, respectively, moved to 1602 and 1618 cm⁻¹, and then to 1595 and 1581 cm⁻¹ in the electrochemical reduction at -1.70 and -2.0 V. The red-shift of the band of the pyridonate ring of bpyO from 1620 to 1581 cm⁻¹ upon two-electron reduction could be associated with a shift of the resonance of Equation (3) towards the pyridonate form.

The $\nu(\text{C}\equiv\text{O})$ band at 1996 cm⁻¹ of [2]⁺ shifts to 1950 cm⁻¹ upon one-electron reduction of the complex at -1.70 V (Figure 5c). The 1950 cm⁻¹ band of [2]⁰ vanishes completely under electrolysis at -2.05 V. Although no new bands assignable to $\nu(\text{C}\equiv\text{O})$ were detected in the region 1800–1900 cm⁻¹, a new band emerged at 1587 cm⁻¹ (Figure 5d). Re-oxidation of the resultant solution at 0 V almost recovered the IR spectrum of [2]⁺ [$\nu(\text{C}\equiv\text{O})$ band at 1996 cm⁻¹].^[16] Thus, the conversion between [2]⁺ and [2]⁻ in CH₃CN is a chemically reversible process, although [2]⁰ undergoes an irreversible reduction at -2.05 V. The 1587 cm⁻¹ band of [2]⁻ is therefore assigned to the stretching mode of the O–C=O moiety of the five-membered metallacycle formed by the attack of the pyridonate oxygen at the carbonyl atom of the CO ligand [Equation (6)].



This reversible ring-closing and -opening [Equation (6)] is also supported by the IR spectra of [2*]⁺, which contains a C¹⁸O ligand. The $\nu(\text{C}\equiv^{18}\text{O})$ band at 1946 cm⁻¹ of [2*]⁺ shifts to 1907 cm⁻¹ and then to 1562 cm⁻¹ upon electrolysis at -1.70 and -2.00 V, respectively (Figure 6). Thus, the 1562 cm⁻¹ band of [2*]⁻ can reasonably be associated with the isotropic shift of the 1587 cm⁻¹ band of [2]⁻. Both [2]⁻

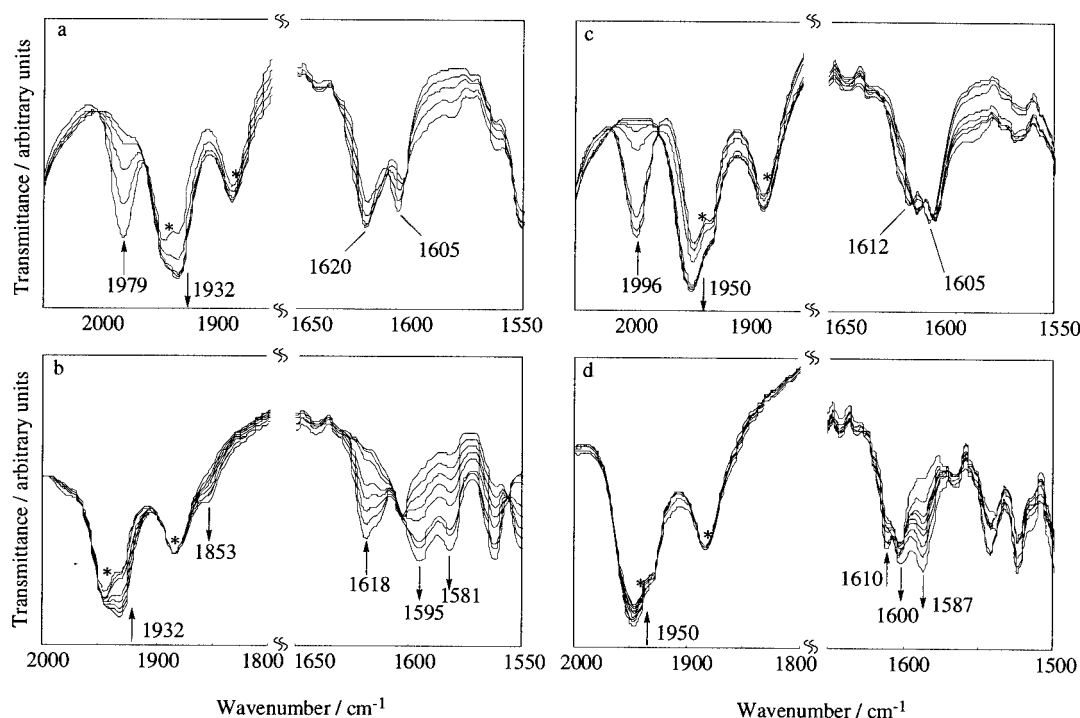


Figure 5. IR spectra of $[1](PF_6)$ (a and b) and $[2](PF_6)$ (c and d) under controlled-potential electrolyses at -1.70 V (a and c) and -2.00 V (b and d) in CD_3CN under N_2 ; * denotes CD_3CN peaks

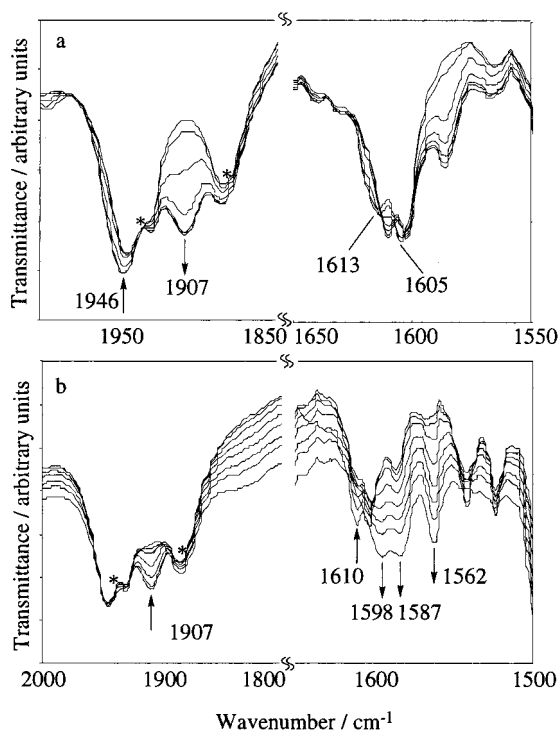


Figure 6. IR spectra of $[2^*](PF_6)$ under controlled potential electrolysis at -1.70 V (a) and -2.00 V (b) in CD_3CN under N_2 ; * denotes CD_3CN peaks

and $[2^*]^-$ exhibit a band at 1587 cm^{-1} . This observation indicates the overlapping of the ring vibration mode of the bpyO moiety of $[2]^-$ with the stretching mode of the $O-C=^{16}O$ group.

As described above, the hydroxyl proton of the bpyOH ligand of $[1H]^{2+}$ and $[2H]^{2+}$ undergoes irreversible reduction at around -1.50 V to form $[1]^+$ and $[2]^+$ in CH_3CN [Equation (5)]. In fact, the electrolysis of $[1H]^{2+}$ and $[2H]^{2+}$ in CH_3CN at -1.40 V causes the disappearance of the $\nu(C\equiv O)$ bands at 1992 and 2005 cm^{-1} of these complexes, and the appearance of the $\nu(C\equiv O)$ bands at 1799 and 1996 cm^{-1} of $[1]^+$ and $[2]^+$, respectively. Although the redox potentials of $[1]^+$ and $[2]^+$ are too negative to evaluate whether the pK_a values of the bpyOH ligand depend on the oxidation states of the complexes, the distinct difference in the Ru–CO bond stability between $[1]^-$ and $[2]^-$ is explained by the cyclometallation due to the intramolecular attack of the oxygen of bpyO at CO in the latter.

Conclusion

We succeeded in selectively synthesizing two isomers ($[1]^+$ and $[2]^+$) with a different orientation of bpyO at the ruthenium center. The hydrogen bond between the pyridonate oxygen and H_2O in $[Ru(terpy)(bpyO)(OH_2)]^+$ may play an important role in the preparation of $[2]^+$. $[1]^+$ and $[2]^+$ can be reversibly converted into $[1H]^{2+}$ and $[2H]^{2+}$ by the protonation of the oxygen atom of bpyO. Based on their pK_a 's, CVs and IR spectra, the electron density at the ruthenium center of $[1]^+$ is higher than that of $[2]^+$. Such a difference is associated with the stronger *trans* influence of CO compared with the central pyridine of terpy, because the electron-withdrawing ability of CO induces the pyridonato

structure of the resonance between metal-pyridinolate and -pyridonate forms [Equation (3)]. The CVs of $[1]^+$ and $[2]^+$ show one reversible and one irreversible redox wave due to terpy- and bpyO-based redox reactions. The two-electron reduction of $[1]^+$ is followed by a partial Ru–CO bond cleavage. On the other hand, the bpyO-based reduction of $[2]^+$ causes cyclometalation by an attack of the pyridonate oxygen at the carbonyl carbon; re-oxidation of the resultant $[2]^-$ almost recovers $[2]^+$. Thus, cyclometallation caused by a bpyO-based reduction effectively suppresses the reductive cleavage of a Ru–CO bond.

Experimental Section

Reagents: 2-Bromo-6-methoxypyridine, 2,2':6',2''-terpyridine and AgPF₆ were purchased from Aldrich Chemical Co., Inc. 2-(Tri-*n*-butylstannyl)pyridine was purchased from Lancaster Synthesis, pyridine hydrochloride from Kanto Chemical Co., Inc., NH₄PF₆ from Wako Pure Chemical Industries, Ltd., and Me₄NBF₄ from Nacalai Tesque. CD₃CN was purchased from Merck (for IR measurements) and Isotec (for NMR measurements). All solvents used for preparations were reagent grade and used without further purification. [Ru(terpy)Cl₃] was prepared according to the literature method.^[17]

Physical Methods: ¹H and ¹H-¹H-COSY NMR experiments were performed with a JEOL LA-500 spectrometer. IR spectra were recorded with a Shimadzu FTIR-8300 spectrophotometer. ESI-MS spectra were measured with a Shimadzu LCMS-2010 liquid chromatograph mass spectrometer. pH titrations were performed with a Hiranuma automatic titrator COM-980 Win. Aqueous solutions (3 mL) of [1H](PF₆)₂ (1.0–1.5 mM) or [2H](PF₆)₂ (1.0–1.5 mM) were titrated with an aqueous NaOH solution (0.1 N, *f* = 1.04) at 25 °C. Cyclic voltammograms were obtained in a one-compartment cell consisting of a glassy carbon working electrode, a platinum counterelectrode and an Ag/AgNO₃ (10 mM) reference electrode in CH₃CN containing Me₄NBF₄ (50 mM) and the complex (1 mM). The cyclic voltammetric data were collected with an ALS/Chi model 1660A electrochemical analyzer. IR spectra under controlled-potential electrolysis conditions were obtained using a thin-layer cell sandwiched between two KBr crystals with an Au mesh working electrode, a platinum wire counterelectrode, and an Ag/AgNO₃ (10 mM) reference electrode.^[3d] The measurements were conducted in CD₃CN or CH₃CN containing the sample complex (10 mM) and Me₄NBF₄ (50 mM) as an electrolyte.

Preparation of 6-Methoxy-2,2'-bipyridine: A toluene solution (35 mL) containing 2-bromo-6-methoxypyridine (1.0 g, 5.32 mmol), 2-(tri-*n*-butylstannyl)pyridine (3.0 g), LiCl (2.2 g, 53 mmol), and [PdCl₂(PPh₃)₂] (290 mg, 0.42 mmol) was deaerated by bubbling N₂ through it. The mixture was then refluxed under N₂ for 18 h, and an aqueous solution (10 mL) of NaF (2.2 g, 53 mmol) was added to the solution at room temperature. The resultant solution was further stirred at ambient temperature for 30 min. An insoluble solid was filtered off, and the filtrate was treated with a 5% Na₂CO₃ aqueous solution in a separating funnel. The organic layer was dried with anhydrous sodium sulfate, and the solvents were evaporated to dryness under reduced pressure. The obtained oil was dissolved in CHCl₃/EtOAc (95:5, v/v), and purified on a silica gel column. Yield: 830 mg (83.7%). The identification of the compound was performed according to the literature (¹H NMR).^[18]

Preparation of 6-Hydroxy-2,2'-bipyridine (bpyOH): A mixture of 6-methoxy-2,2'-bipyridine (700 mg, 3.76 mmol) and pyridine hydrochloride (10 g) was heated under N₂ at 210 °C for 90 min. After the reaction mixture had cooled to ambient temperature, the white solid that appeared was dissolved in H₂O (50 mL). The crude product was extracted from the aqueous solution with dichloromethane. The dichloromethane layer was further treated with a saturated aqueous NaHCO₃ solution. The organic layer was dried with anhydrous sodium sulfate, and the solvents were evaporated to dryness under reduced pressure. Recrystallization from CH₂Cl₂/hexane (1:1, v/v) gave a pale-yellow solid. Yield 520 mg (80.4%). The identification of the compound was performed according to the literature (¹H NMR).^[19]

Preparation of [Ru(terpy)(bpyOH)Cl]Cl·H₂O: BpyOH (40 mg, 0.23 mmol) and Et₃N (120 mg, 1.18 mmol) were added to a suspension of [Ru(terpy)Cl₃] (100 mg, 0.22 mmol) in 2-methoxyethanol. The mixture was stirred under N₂ at 85 °C for 3 h, during which time the suspension gradually changed to a deep purple solution. After an insoluble solid was filtered off, the filtrate was concentrated to about 5 mL under reduced pressure. The resultant precipitate was separated by filtration and recrystallized from methanol. Yield 65 mg (49.6%). C₂₅H₂₁Cl₂N₅O₂Ru: calcd. C 50.42, H 3.55, N 11.76; found C 49.98, H 3.47, N 11.60. ESI-MS: *m/z* = 542 [Ru(terpy)(bpyOH)Cl]⁺.

Preparation of [Ru(terpy)(bpyO)(CO)](PF₆)₂ {1I}(PF₆)₂: A mixture of [Ru(terpy)(bpyOH)Cl]Cl·H₂O (90 mg, 0.15 mmol) and AgPF₆ (81 mg, 0.32 mmol) in 2-methoxyethanol was stirred under CO pressure (15 atm) at 85 °C for 24 h. After the solution had cooled to room temperature, the solution was filtered through a Celite layer to remove the AgCl precipitate and then concentrated to about 5 mL. Addition of an excess amount of an aqueous NH₄PF₆ solution gave a yellow precipitate, which was separated by filtration. The resultant product was recrystallized from acetone/ethanol (2:1, v/v) containing Et₃N (30 μL). Yield 100 mg (53.6%). ¹H NMR (500 MHz, CD₃CN): δ = 5.65 (d, 1 H, H^{A3}), 6.98 (d, 1 H, H^{A5}), 7.08 (dd, 1 H, H^{A4}), 7.39 (ddd, 2 H, H^{C4}), 7.61 (ddd, 1 H, H^{B5}), 7.69 (d, 2 H, H^{C3}), 8.05 (td, 2 H, H^{C5}), 8.09 (td, 1 H, H^{B4}), 8.21 (t, 1 H, H^{D4}), 8.26 (d, 1 H, H^{B3}), 8.31 (m, 4 H, H^{C6} and H^{D3}), 9.35 (d, 1 H, H^{B6}) ppm. C₂₆H₁₈F₆N₅O₂PRu: calcd. C 46.03, H 2.67, N 10.32; found C 45.86, H 2.79, N 10.33. ESI-MS: *m/z* = 534 [Ru(terpy)(bpyO)(CO)]⁺.

Preparation of [Ru(terpy)(bpyOH)(CO)](PF₆)₂ {1H}(PF₆)₂: Yellow crystals of [1H](PF₆)₂ were obtained by crystallization of [1I](PF₆)₂ from CH₃CN/H₂O (1:1, v/v) containing 1.5 equiv. of an aqueous HPF₆ solution (1 M). ¹H NMR (500 MHz, CD₃CN): δ = 6.97 (d, 1 H, H^{A3}), 7.41 (ddd, 2 H, H^{C4}), 7.68 (d, 2 H, H^{C3}), 7.76 (dd, 1 H, H^{A4}), 7.79 (ddd, 1 H, H^{B5}), 7.90 (d, 1 H, H^{A5}), 8.11 (td, 2 H, H^{C5}), 8.26 (td, 1 H, H^{B4}), 8.38 (t, 1 H, H^{D4}), 8.43 (d, 2 H, H^{C6}), 8.47 (d, 2 H, H^{D3}), 8.51 (d, 1 H, H^{B3}), 9.45 (d, 1 H, H^{B6}) ppm. ESI-MS: *m/z* = 267.5 [Ru(terpy)(bpyOH)(CO)]²⁺.

Preparation of [Ru(terpy)(bpyO)(OH₂)](PF₆)₂: Na₂CO₃ (91 mg, 0.86 mmol) and Et₃N (0.4 mL) were added to a suspension of [Ru(terpy)Cl₃] (250 mg, 0.57 mmol) in MeOH/H₂O (1:2 v/v, 80 mL), and then the suspension was refluxed under N₂ for 150 min. The resultant solution was cooled to room temperature, filtered, and the filtrate was concentrated to dryness under reduced pressure. The resulting solid was dissolved in ethanol and any insoluble salt was removed by filtration. Then, the solution was concentrated to dryness, and the solid was purified by column chromatography on a Cosmosil column, with MeOH as eluent. An aqueous solution

(5 mL) of [Ru(terpy)(CO₃)(OH₂)] (60 mg) and bpyOH (30 mg, 0.17 mmol) was stirred at ambient temperature for 2–3 d, and the solution was then filtered. Addition of an excess amount of NH₄PF₆ to the filtrate gave [Ru(terpy)(bpyO)(OH₂)](PF₆) as a red-purple powder which was isolated by filtration, and recrystallized from acetone/H₂O (4:1, v/v). Yield 45 mg (11.8%). ¹H NMR (500 MHz, [D₆]acetone): δ = 6.71 (d, 1 H, H^{A3}), 6.89 (ddd, 1 H, H^{B4}), 7.30 (d, 1 H, H^{B3}), 7.56 (ddd, 2 H, H^{C4}), 7.62 (td, 1 H, H^{B5}), 7.67 (d, 1 H, H^{A5}), 7.79 (t, 1 H, H^{A4}), 8.05 (td, 2 H, H^{C5}), 8.11 (d, 2 H, H^{C3}), 8.20–8.25 (m, 2 H, H^{B6} and H^{D4}), 8.64 (d, 2 H, H^{C6}), 8.76 (d, 2 H, H^{D3}) ppm. C₂₅H₂₀F₆N₅O₂PRu: calcd. C 44.92, H 3.01, N 10.48; found C 45.16, H 3.20, N 10.44. ESI-MS: m/z = 524 [Ru(terpy)(bpyO)(OH₂)]⁺.

Preparation of [Ru(terpy)(bpyO)(CO)](PF₆)·H₂O {2}(PF₆)·H₂O: A 2-methoxyethanol solution of [Ru(terpy)(bpyO)(OH₂)](PF₆) (45 mg, 0.07 mmol) was stirred under CO pressure (20 atm) at 90 °C for 12 h. The reaction mixture was then concentrated to about 5 mL under reduced pressure. Addition of an excess amount of an aqueous NH₄PF₆ solution to the solution gave an orange precipitate, which was separated by filtration. Orange crystals were obtained by vapor diffusion of diethyl ether into an EtOH solution containing Et₃N (15 μ L). Yield 22 mg (44.9%). ¹H NMR (500 MHz, CD₃CN): δ = 6.60 (d, 1 H, H^{A3}), 7.00 (d, 1 H, H^{B3}), 7.05 (ddd, 1 H, H^{B4}), 7.24 (d, 1 H, H^{A5}), 7.45 (ddd, 2 H, H^{C4}), 7.54 (dd, 1 H, H^{A4}), 7.81 (td, 1 H, H^{B5}), 7.90 (d, 2 H, H^{C3}), 8.07 (td, 2 H, H^{C5}), 8.12 (d, 1 H, H^{B6}), 8.39 (d, 2 H, H^{C6}), 8.42 (t, 1 H, H^{D4}), 8.54 (d, 2 H, H^{D3}) ppm. C₂₆H₂₀F₆N₅O₃PRu: calcd. C 44.83, H 2.89, N 10.05; found C 44.71, H 2.93, N 10.09. ESI-MS: m/z = 534 [Ru(terpy)(bpyO)(CO)]⁺.

Preparation of [Ru(terpy)(bpyOH)(CO)](PF₆)₂·2H₂O {2H}(PF₆)₂·2H₂O: Orange crystals of 2H(PF₆)₂·2H₂O were obtained by crystallization of 2(PF₆) from CH₃CN/H₂O (1:1, v/v) containing 1.5 equiv. of an aqueous HPF₆ solution (1 M). ¹H NMR (500 MHz, CD₃CN): δ = 7.14 (d, 1 H, H^{B3}), 7.27 (ddd, 1 H, H^{B4}), 7.42–7.45 (m, 3 H, H^{A3} and H^{C4}), 7.80 (d, 2 H, H^{C3}), 8.01 (td, 1 H, H^{B5}), 8.10–8.20 (m, 4 H, H^{A4}, H^{A5} and H^{C5}), 8.38 (d, 1 H, H^{B6}), 8.43 (d, 2 H, H^{C6}), 8.51 (t, 1 H, H^{D4}), 8.58 (d, 2 H, H^{D3}) ppm.

C₂₆H₂₃F₁₂N₅O₄P₂Ru: calcd. C 36.29, H 2.69, N 8.14; found C 36.26, H 2.80, N 8.13. ESI-MS: m/z = 267.5 [Ru(terpy)(bpyOH)(CO)]²⁺.

Preparation of [Ru(terpy)(bpyO)(C¹⁸O)](PF₆) {2*}(PF₆): Et₃N (0.1 equiv.) was added to a CH₃CN/H₂¹⁸O (4:1, v/v, 1 mL) solution of 2(PF₆) (40 mg) and the mixture was heated at 50 °C for 2 d. After the solution had cooled to room temperature, the solvent was removed completely. The orange solid thus obtained was recrystallized from CH₃CN/EtOH (1:4, v/v). The purity of the complex was checked by comparison of the parent peaks of m/z = 534 ([2]⁺) and 536 ([2*]⁺) in the ESI-MS, and of the ν (C¹⁶O) and ν (C¹⁸O) bands at 1996 and 1946 cm⁻¹ in the IR spectra. Based on these results, the sample used in the experiments contained about 80% [2*](PF₆) and 20% [2](PF₆). Yield 18 mg. ESI-MS: m/z = 536 [Ru(terpy)(bpyO)(C¹⁸O)]⁺.

Crystallographic Study of [Ru(terpy)(bpyO)(OH₂)](PF₆), [1](PF₆), [2](PF₆)·H₂O, and [2H](PF₆)₂·2H₂O: Crystals for X-ray analyses of the complexes were obtained as described above. A suitable single crystal for the measurement was mounted on a glass fiber. Data were collected at -100 °C on a Rigaku/MSC Mercury CCD diffractometer with graphite-monochromated Mo-*K*_α radiation (λ = 0.71070 Å). All data were collected and processed using the Crystal Clear program (Rigaku). All the calculations were carried out with the teXsan software package.^[20] All structures were solved by direct methods and expanded using Fourier techniques. Refinements were performed anisotropically for all non-hydrogen atoms by the full-matrix least-squares method. Hydrogen atoms were placed at the calculated positions and were included in the structure calculation without further refinement of the parameters. Crystal data and processing parameters are summarized in Table 3. CCDC-240927 for [Ru(terpy)(bpyO)(OH₂)](PF₆), -217817 for [1](PF₆), -217818 for [2](PF₆)·H₂O and -217819 for [2H](PF₆)₂·2H₂O contain the supplementary crystallographic data for this paper. These data can be obtained free of charge at www.ccdc.cam.ac.uk/conts/retrieving.html [or from the Cambridge Crystallographic Data Centre, 12 Union Road, Cambridge CB2 1EZ, UK; Fax: + 44-1223-336-033; E-mail: deposit@ccdc.cam.ac.uk].

Table 3. Crystallographic data for [Ru(terpy)(bpyO)(OH₂)](PF₆), [1](PF₆), [2](PF₆)·H₂O and [2H](PF₆)₂·2H₂O

| | [Ru(terpy)(bpyO)(OH ₂)](PF ₆) | [1](PF ₆) | [2](PF ₆)·H ₂ O | [2H](PF ₆) ₂ ·2H ₂ O |
|-------------------------------------------------|----------------------------------------------------------------------------------|----------------------------------------------------------------------------------|----------------------------------------------------------------------------------|-------------------------------------------------------------------------------------------------|
| Empirical formula | C ₂₅ H ₂₀ F ₆ N ₅ O ₂ PRu | C ₂₆ H ₁₈ F ₆ N ₅ O ₂ PRu | C ₂₆ H ₂₀ F ₆ N ₅ O ₃ PRu | C ₂₆ H ₂₃ F ₁₂ N ₅ O ₄ P ₂ Ru |
| Formula mass | 668.50 | 678.49 | 696.51 | 860.50 |
| Crystal system | monoclinic | monoclinic | orthorhombic | triclinic |
| Space group | <i>P</i> 2 ₁ / <i>n</i> | <i>C</i> 2/ <i>c</i> | <i>Pca</i> 2 ₁ | <i>P</i> $\bar{1}$ |
| Color | red purple | orange | orange | orange |
| <i>a</i> [Å] | 10.413(1) | 41.034(3) | 15.457(1) | 8.6983(4) |
| <i>b</i> [Å] | 14.505(1) | 8.5910(5) | 16.176(1) | 14.0966(1) |
| <i>c</i> [Å] | 16.601(1) | 14.349(1) | 11.3332(8) | 14.8504(2) |
| α [°] | | | | 62.952(9) |
| β [°] | 98.593(4) | 95.404(3) | | 78.28(1) |
| γ [°] | | | | 84.67(1) |
| <i>V</i> [Å ³] | 2479.3(4) | 5036.0(6) | 2833.7(6) | 1587.9(2) |
| <i>Z</i> | 4 | 8 | 4 | 2 |
| <i>D</i> _{calcd} [g·cm ⁻³] | 1.791 | 1.790 | 1.623 | 1.80 |
| Crystal size [mm] | 0.30 × 0.15 × 0.10 | 0.20 × 0.20 × 0.10 | 0.25 × 0.13 × 0.06 | 0.40 × 0.20 × 0.10 |
| <i>T</i> [K] | 173 | 173 | 173 | 173 |
| λ [Å] | 0.71070 | 0.71070 | 0.71070 | 0.71070 |
| μ [mm ⁻¹] | 0.778 | 0.768 | 0.687 | 0.708 |
| <i>R</i> ₁ [a] | 0.067 | 0.048 | 0.070 | 0.079 |
| <i>R</i> _w [b] | 0.153 | 0.108 | 0.176 | 0.201 |

[a] $R_1 = \sum |F_o| - |F_c| / \sum |F_o|$ for $I > 2.0\sigma(I)$ data. [b] $R_w = \sum [w(F_o^2 - F_c^2)^2 / \sum w(F_o^2)^2]^{1/2}$.

- [1] [1a] M. Suzuki, C. C. Waraksa, T. E. Mallouk, H. Nakayama, K. Hanabusa, *J. Phys. Chem. B* **2002**, *106*, 4227. [1b] M. Osawa, M. Hoshino, Y. Wakatsuki, *Angew. Chem. Int. Ed.* **2001**, *40*, 3472. [1c] S. Fanni, F. M. Weldon, L. Hammarström, E. Mukhtar, W. R. Browne, T. E. Keyes, J. G. Vos, *Eur. J. Inorg. Chem.* **2001**, 529. [1d] B. Saha, D. M. Stanbury, *Inorg. Chem.* **2000**, *39*, 1294. [1e] C. Nasr, S. Hotchandani, P. V. Kamat, *J. Phys. Chem. B* **1998**, *102*, 4944. [1f] T. Rajendran, S. Rajagopal, C. Srinivasan, P. Ramamurthy, *J. Chem. Soc., Faraday Trans.* **1997**, *93*, 3155. [1g] J.-P. Sauvage, J.-P. Collin, J.-C. Chambron, S. Guillelre, C. Coudret, *Chem. Rev.* **1994**, *94*, 993. [1h] R. Argazzi, C. A. Bignozzi, T. A. Heimer, F. N. Castellano, G. J. Meyer, *Inorg. Chem.* **1994**, *33*, 5741. [1i] Y. I. Kim, S. J. Atherton, E. S. Brigham, T. E. Mallouk, *J. Phys. Chem.* **1993**, *97*, 11802.
- [2] [2a] H. Ishida, T. Terada, K. Tanaka, T. Tanaka, *Inorg. Chem.* **1990**, *29*, 905. [2b] J. M. Lehn, R. Ziessel, *J. Organomet. Chem.* **1990**, *382*, 157. [2c] H. Ishida, K. Tanaka, T. Tanaka, *Chem. Lett.* **1988**, 339. [2d] H. Ishida, K. Tanaka, T. Tanaka, *Chem. Lett.* **1987**, 1035. [2e] J. Hawecker, J. Lehn, R. Ziessel, *J. Chem. Soc., Chem. Commun.* **1985**, 56.
- [3] [3a] S. Chardon-Noblat, G. H. Cripps, A. Deronzier, J. S. Field, S. Gouws, R. J. Haines, F. Southway, *Organometallics* **2001**, *20*, 1668. [3b] S. Chardon-Noblat, A. Deronzier, R. Ziessel, D. Zsoldos, *Inorg. Chem.* **1997**, *36*, 5384. [3c] R. Ziessel, L. Toupet, S. Chardon-Noblat, A. Deronzier, D. Matt, *J. Chem. Soc., Dalton Trans.* **1997**, 3777. [3d] H. Nakajima, Y. Kushi, H. Nagao, K. Tanaka, *Organometallics* **1995**, *14*, 5093. [3e] H. Nagao, T. Mizukawa, K. Tanaka, *Inorg. Chem.* **1994**, *33*, 3415. [3f] M. N. Collomb-Dunand-Sauthier, A. Deronzier, R. Ziessel, *J. Chem. Soc., Chem. Commun.* **1994**, 189. [3g] M. N. Collomb-Dunand-Sauthier, A. Deronzier, R. Ziessel, *Inorg. Chem.* **1994**, *33*, 2961. [3h] S. Chardon-Noblat, M. N. Collomb-Dunand-Sauthier, A. Deronzier, R. Ziessel, D. Zsoldos, *Inorg. Chem.* **1994**, *33*, 4410. [3i] J. R. Pugh, M. R. M. Bruce, B. P. Sullivan, T. J. Meyer, *Inorg. Chem.* **1991**, *30*, 86. [3j] H. Ishida, K. Tanaka, T. Tanaka, *Organometallics* **1987**, *6*, 181. [3k] C. M. Bolinger, B. P. Sullivan, D. Conrad, J. A. Gilbert, N. Story, T. J. Meyer, *J. Chem. Soc., Chem. Commun.* **1985**, 796.
- [4] [4a] S.-L. Zheng, J.-P. Zhang, W.-T. Wong, X.-M. Chen, *J. Am. Chem. Soc.* **2003**, *125*, 6882. [4b] X.-M. Zhang, M.-L. Tong, M.-L. Gong, H.-K. Lee, L. Luo, K.-F. Li, Y.-X. Tong, X.-M. Chen, *Chem. Eur. J.* **2002**, *8*, 3187. [4c] X.-M. Zhang, M.-L. Tong, X.-M. Chen, *Angew. Chem. Int. Ed.* **2002**, *41*, 1029. [4d] S. Mukhopadhyay, R. J. Staples, W. H. Armstrong, *Chem. Commun.* **2002**, 864. [4e] G. Y. S. K. Swamy, K. C. Mohan, K. Ravikumar, *Cryst. Res. Technol.* **2001**, *36*, 615.
- [5] H. Nakajima, K. Tanaka, *Chem. Lett.* **1995**, 891.
- [6] [6a] P. Nombel, N. Luga, B. Donnadieu, G. Lavigne, *Organometallics* **1999**, *18*, 187–196. [6b] O. C. P. Beers, J. G. P. Delis, W. P. Mul, K. Vrieze, C. J. Elsevier, *Inorg. Chem.* **1993**, *32*, 3640. [6c] M. Nonoyama, *Polyhedron* **1985**, *4*, 765.
- [7] [7a] A. L. Jorgenson, R. A. Nadeau, V. G. Young Jr, W. L. Gladfelter, *J. Organomet. Chem.* **1998**, *563*, 1. [7b] M. Wijnkoop, P. P. M. Lange, H.-W. Fruhauf, K. Vrieze, *Organometallics* **1995**, *14*, 4781. [7c] M. Wijnkoop, P. P. M. Lange, H.-W. Fruhauf, K. Vrieze, *Organometallics* **1992**, *11*, 3607. [7d] N. G. Connolly, M. J. Freeman, I. Manners, A. G. Orpen, *J. Chem. Soc., Dalton Trans.* **1984**, 2703.
- [8] The orientation of the bpyOH group in [Ru(terpy)-(bpyOH)Cl]⁺ was determined unequivocally by the X-ray crystal structure analysis but the quality of the crystals of the complex was not enough to allow a discussion of the bond angles and lengths ($R_1 = 11.8\%$, $R_w = 20.5\%$).
- [9] E. P. Kelson, P. P. Phengsy, *J. Chem. Soc., Dalton Trans.* **2000**, 4023.
- [10] L. S. Hollis, S. J. Lippard, *Inorg. Chem.* **1983**, *22*, 2708.
- [11] C. R. Hecker, P. E. Fanwick, D. R. McMillin, *Inorg. Chem.* **1991**, *30*, 659.
- [12] The controlled-potential electrolysis of [1]⁺ and [2]⁺ at –1.80 V revealed that both complexes undergo one-electron reduction ($n = 1.0$) at the first cathodic wave. The potentials of the second cathodic waves of both complexes are too negative to determine the number of electrons by controlled-potential electrolysis. Based on the comparison of the peak currents of the first and the second waves of the complexes, both [1]⁰ and [2]⁰ are supposed to undergo one-electron reduction at the second cathodic wave.
- [13] [13a] N. E. Tokel-Takvoryan, R. E. Hemingway, A. J. Bard, *J. Am. Chem. Soc.* **1973**, *95*, 6582. [13b] J. M. Calvert, T. J. Meyer, *Inorg. Chem.* **1981**, *20*, 27. [13c] B. Jing, W. Wang, M. Zhang, T. Shen, *Dyes Pigm.* **1998**, *37*, 177.
- [14] The third cathodic wave of [1H]²⁺ ($E_{p,c} = -1.85$ V) was not assigned.
- [15] A poorly resolved peak at about –1.40 V in the CV of [2H]²⁺ (Figure 4b) results from H₂ evolution [Equation (5)]. Accordingly, addition of Et₃N to the solution converts [2H]²⁺ to [2]⁺. As a result, the pattern of the CV was sharpened and the irreversible cathodic wave of Et₄NH⁺ was observed at –1.75 V.
- [16] The first and second reductions of [2]⁺ are associated with terpy- and bpyO-localized redox reactions, respectively. The second reduction causes metallocyclization of the complex. However, the oxidation processes of [1][–] and [2][–] are not clearly observed in the CV (Figure 3). The electrochemical oxidation of those two-electron-reduced complexes, therefore, was conducted at 0 V.
- [17] B. P. Sullivan, J. M. Calvert, T. J. Meyer, *Inorg. Chem.* **1980**, *19*, 1404.
- [18] [18a] P. Gros, Y. Fort, *Synthesis* **1999**, 754. [18b] P. M. Pojer, L. A. Summers, *J. Heterocycl. Chem.* **1974**, *11*, 303.
- [19] S. Rozen, D. Hebel, *Heterocycles* **1989**, *28*, 249.
- [20] *teXsan, Crystal Structure Analysis Package*, version 1.11, Molecular Structure Corporation, Rigaku Corporation, 2000.

Received June 16, 2004

Early View Article

Published Online December 2, 2004